FoamVis: Visualization of 2D Foam Simulation Data

Dan R. Lipşa, Robert S. Laramee, Simon J. Cox, I. Tudur Davies

Abstract—Research in the field of complex fluids such as polymer solutions, particulate suspensions and foams studies how the flow of fluids with different material parameters changes as a result of various constraints. Surface Evolver, the standard solver software used to generate foam simulations, provides large, complex, time-dependent data sets with hundreds or thousands of individual bubbles and thousands of time steps. However this software has limited visualization capabilities, and no foam specific visualization software exists. We describe the foam research application area where, we believe, visualization has an important role to play. We present a novel application that provides various techniques for visualization, exploration and analysis of time-dependent 2D foam simulation data. We show new features in foam simulation data and new insights into foam behavior discovered using our application.

Index Terms—Surface Evolver, bubble-scale simulation, time-dependent visualizations

1 Introduction and Motivation

Liquid foams have many important domestic and industrial uses including fire fighting, oil recovery, mineral separation processes, sanitation and food and beverage production [31]. Two foam applications directly related to the simulations visualized in this work are oil recovery and mineral flotation and separation. In the former case, it is required to know how the constricted geometry of the porous rock, in which the oil resides, affects the passage of the foam that acts to displace it, and whether blocked regions develop. In the latter case, the efficiency of the separation process is determined by the way in which solid objects in the foam move, under gravity, and in particular whether they can be carried by the foam and collected for further processing and purification.

In contrast to solid foams constructed from, for example, aluminum or polyurethane, liquid foams evolve in time, presenting a more difficult challenge for visualization. An important parameter is the liquid fraction, which indicates where a given foam lies between the limits of a dry foam, in which the liquid walls of the structure (soap films) are thin and the gas bubbles polyhedral, and a wet foam, in which the gas bubbles are spherical. Foams minimize their surface energy, equivalent to area, which means that at equilibrium they satisfy Plateau's [22] geometric laws.

Physicists use simulation to study basic properties of foam that are still not well understood. For example, can the path that a bubble traverses be predicted? How do bubbles and soap films behave under stress and shear? To what extent do objects falling through a foam interact [7]? Does the whole foam flow when pushed through a constricted geometry? Surface Evolver (SE) [4] is the *de facto* standard for studying these questions because it can be used for foam simulations at the bubble-scale, which are the most accurate both in terms of structure and flow. Researching SE foam simulations poses special challenges:

1. Access to simulation data is difficult and requires domain specific knowledge. Parsing and special processing are required to access the full simulation data. Important bubble attributes are not provided by the simulation but inferred using domain specific knowledge.

2. Triggers to various foam behaviors are difficult to infer. Multiple attributes have to be examined and foam properties have to be taken into account. Topological changes (T1s), in which bubbles swap neighbors, have to be considered.

3. It is challenging to visualize general foam behavior. While bubble-scale simulation makes it possible to investigate the influences that material properties have on general foam behavior, it makes it difficult to visualize the general behavior that is of primary interest. Simulation data is complex (unstructured grid with polygonal cells) and time dependent, with large fluctuations in the values of the parameters determined by changes in the topology of the soap film network (T1s).

4. The most difficult challenge and the goal of foam research is to discover how general foam behavior depends on foam properties such as bubble size, distribution and liquid fraction.

These challenges make it difficult to use a general purpose visualization tool for foam simulations. Domain experts' visualizations only partially address these challenges. They may require intervention in the simulation code and potentially recomputing the simulations for summarizing and saving the relevant data. Their standard visualizations do not have the ability to explore and analyze the data through navigation, selection and encoding operations. They do not have the high level of detail and speed that is achieved using graphics hardware. We address shortcomings of existing visualizations used by domain experts and we provide visualizations to address foam research challenges. To the best of our knowledge, no visualization software exists for foam simulations modeled with SE. FoamVis fills this void by providing a comprehensive solution which facilitates advanced examination and analysis of foam simulation data. Specifically, our work makes the following contributions:

- We describe foam research as an application area. We believe visualization can play an important role in understanding foam response to various stimuli which in turn can benefit many practical applications.

- We describe novel visualization solutions for analyzing the results of a foam simulation performed at the bubble-scale using Surface Evolver (SE). We show how our solutions are driven by foam visualization challenges. Our tool can be used in other areas of the physical sciences where SE is used for simulation. Examples include the study of emulsions [23] or solder in electronic circuits [5, 13].

- We show how scientists using our tool make new discoveries, validate hypotheses, and gain insights into foam behavior.

The rest of this paper is organized as follows: Section 2 presents related work, Section 3 presents foam research background information and a short description of the simulation datasets used in this work. We present visualization techniques used to inspect and analyze foam

- *Dan R. Lipşa and Robert S. Laramee are with Swansea University, E-mails: {d.lipsa, r.s.laramee}@swansea.ac.uk*
- *Simon J. Cox and I. Tudur Davies are with Aberystwyth University, E-mails: {foams, itd}@aber.ac.uk*

Manuscript received 31 March 2011; accepted 1 August 2011; posted online 23 October 2011; mailed on 14 October 2011.
For information on obtaining reprints of this article, please send email to: tvcg@computer.org.

data in Section 4. We present insights gathered and discoveries made using our tool in Section 5. We end with conclusions and future work in Section 6.

2 Related Work

In our survey of the literature [19], very little work in visualization of time-dependent, physically accurate foam simulation data has been published. We present related works that visualize static foam structures. Bigler et al. [2] explain and evaluate two methods of augmenting the visualization of particle data using ambient occlusion and silhouette edges. They visualize a foam data set acquired using micro-CT by converting it first to a particle distribution and then using an interactive ray-tracer for rendering. König et al. [18] present an interactive tool to investigate the structure of metal foam. They employ techniques for real-time isosurface rendering, determine the isosurface threshold value such that the volume of the computed foam sample matches the real-world sample and render cells with certain size and shape criteria. Hadwiger et al. [12] present a method for interactive exploration of industrial CT volumes such as cast metal parts. They detect and classify defects in a material using interactive exploration instead of an offline process of setting parameters and then waiting for the results. These works focus on visualization of static foam or foam-like structures, while our work presents visualization of time-dependent foam simulations.

Computer graphics researchers are also interested in rendering soap bubbles [9, 10, 29], foam [25] and water sprays [20]. However, they simulate and render the appearance of natural phenomena while avoiding the large computational cost of physically accurate simulations.

Ours is the first work of its kind (to our knowledge) to focus on visualization of time-dependent foam simulation data.

3 Foam Research

This section presents background information about foam and its simulation, then it describes two simulations studied with our visualization tool. We outline questions to which foam scientists seek answers, both in general and specifically for the presented simulations. We conclude by presenting existing visualization methods that foam scientists use to analyze foam simulations.

3.1 Background

An aqueous foam is a two-phase material, for example detergent-laden water and air, yet its response can often be solid-like. To accurately predict the rheological properties of foams, including stiffness (shear modulus) and viscosity as well as the complex response described in Equation (1), requires a treatment that differs from the usual methods for predicting fluid flow. The solid-like properties are often attributed to a shear modulus, defined as the derivative of stress with respect to strain. Plasticity is described by a yield stress σ_y, that is, a critical applied stress σ below which the material does not flow, and then fluid-like properties are captured by an effective viscosity, defined loosely as stress divided by strain rate $\dot{\gamma}$. Both the yield stress and the rate of strain are part of the Herschel Bulkley constitutive relation, well-known in the field of complex fluids:

$$\begin{cases} \dot{\gamma} = 0 & \sigma \leq \sigma_y \\ \sigma = \sigma_y + K\dot{\gamma}^n & \sigma > \sigma_y \end{cases}, \tag{1}$$

where K (consistency) and $0 < n \leq 1$ (power-low exponent) are fitting parameters [8, 16]. Such an expression for the stress can now be implemented in a number of commercial CFD packages as a generalized Newtonian model. What is unclear in this approach is the dependence of the parameters K and n on material properties, for example bubble size (and its distribution) and liquid fraction.

A possible solution simulates foams at the bubble scale, where these contributions can be teased out [6]. Surface Evolver (SE) allows a precise representation of the bubbles based upon the observation that a soap film minimizes its surface area. In contrast to other methods, SE can span a large range of liquid fractions and allows for the container geometry to be varied. It is the only standard method that allows the bubble pressures to be calculated, because of its precision. Indeed, where accuracy is required, both in terms of static structure and rheology/flow, SE is the *de facto* standard for foam simulation.

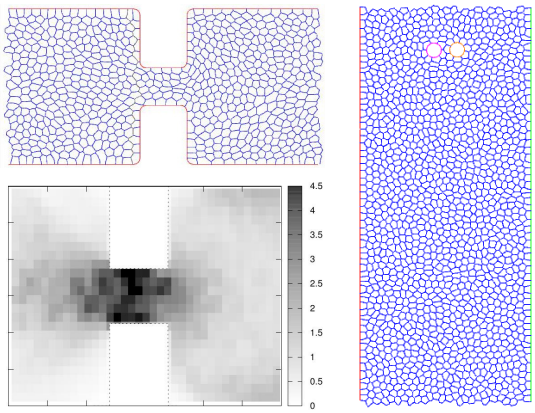

Fig. 1. Typical visualizations used by the domain experts. Images are visualizations of the simulation of foam flow through a constriction [15] and of the simulation of two discs falling through a foam [7]. The left-top image shows an instantaneous image of the foam flowing through a constriction. The left-bottom image shows velocity magnitude averaged over all time steps over a 60x30 grid. The right image shows time step $t = 0$ of the discs falling through a foam simulation.

A challenge of using SE to simulate foam behavior, at least for bulk flows (flow far from the walls of the foam container), is to be able to simulate a sufficiently large number of bubbles to accurately reflect reality. Thus, many simulations are performed in two dimensions, where simulation time scales with the number of bubbles slightly greater than linear [32]. Fortuitously, a good approximation to a two-dimensional foam can also be made experimentally, for example by squeezing bubbles between parallel glass plates [26] or using the Bragg bubble raft [3], thus providing a means to validate simulations. In this two-dimensional setting, there are many opportunities for visualization, as described here.

3.2 Simulation Cases

To present the features of our application we use two simulation cases: the simulation of foam flow through a constriction (*constriction*) and the simulation of sedimenting discs (*sedimenting-discs*). Our application, however, can process any Surface Evolver simulation, both static and dynamic. We present a short description of each simulation. *Constriction* (Fig. 1 left) simulates a 2D polydisperse (bubbles with different volumes) foam flowing through a constricted channel. It has 1000 time steps and simulates 704 bubbles. This simulation subjects foam to different kinds of stress simultaneously and is therefore a testing ground from which to validate the approximations in the model against experiment. *Sedimenting-discs* (Fig. 1 right) simulates two discs falling through a monodisperse (bubbles having equal volume) foam under gravity. It contains 252 time steps and simulates 1500 bubbles. There are two forces on each disc in addition to its weight: a pressure force results from each adjacent bubble pushing against it, while a network force arises because each contacting soap film pulls normal to the circumference with the force of surface tension. Due to the flow, the distribution of films and bubbles pressures around each disc is not uniform (for example, there is a high density of films above each disc, leading to a large, upward, network force there), resulting in a non-zero resultant force.

The two discs are initially side by side and close together. As they fall, they interact with each other by rotating towards a stable orientation in which their line of centers is parallel to gravity. This is a variation of the classic Stokes experiment that is used to probe the rheology of a 2D foam, and for which there is a great deal of experimental data. These simulations are relevant to industrial processes in separation and oil recovery [31].

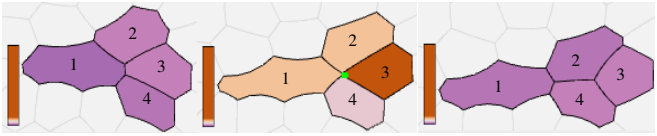

Fig. 2. Topological change (T1 event). The three images show time steps t=20, t=72 and t=73 in the *constriction* simulation. A T1 event can be observed between the bubbles color-mapped by velocity magnitude. In the left image bubbles meet only at three-fold junctions, with bubbles 1 and 3 touching. The four bubbles move to an unstable configuration in which they meet at a four-fold junction in the middle image. Note the high velocity that bubbles have after the T1 event. The right image shows the four bubbles after the T1 event where now bubbles 2 and 4 touch.

3.3 Simulation Method

A dry 2D foam at equilibrium consists of gas bubbles surrounded by films that, as a consequence of energy minimization, are circular arcs which meet threefold at angles of 120°. The foams total energy is equal to the total film length multiplied by the surface tension.

The initial structure for each simulation is created from a Voronoi tessellation of the unit square, with random seeds and periodic boundary conditions. Bubbles are removed from two opposite sides to leave a structure which is only periodic in one direction, with vertices fixed to solid walls in the other direction (Fig. 1). The domain scientists use the Surface Evolver, a finite element code, in a mode in which each film is represented as a circular arc, to find a realistic foam structure by minimizing the total film length subject to the prescribed bubble areas.

During this minimization, topological changes (T1s) (Fig. 2) are triggered by deleting each film that shrinks below a critical cut-off length l_c and allowing a new film to form in a perpendicular direction to complete the process. The critical length l_c is a measure of the effective liquid fraction F.

To apply a pressure gradient to the foam, a line of films spanning the channel is moved downstream by a small distance (constriction). A sedimenting disc is moved a small distance in the direction of the resultant force on it. In both cases, this motion is followed by a reduction of the film length to a local minimum (in the sedimenting discs simulation, the discs are fixed during the minimization). Either non-slip (films attached to the wall do not move because of high friction; sedimenting-discs) or free slip (no resistance to motion along the wall; constriction) boundary conditions can be applied at the channel walls. In this way, the foam passes through a sequence of equilibrium states, appropriate to an applied strain with strain rate much lower than the rate of equilibration after T1s.

3.4 Foam Research Questions

Foam scientists' main goal is to develop a model that successfully predicts foam behavior from measurable properties such as bubble size, disorder and liquid fraction. It is the aim of simulations to identify and separate the influences of these properties on foam response. Matching simulated foam behavior with experiments provides validation for the simulations.

We outline specific questions that foam scientists try to answer about the presented simulations. For the simulation of foam flow through a constricted channel important questions include: For what range of parameters can recirculation zones be found in the upstream corners? That is, are there regions where bubbles are trapped and move in circles (or not at all) rather than downstream, therefore not contributing to the transport of material? What is the pressure drop required to force the flow through a given constricted geometry? Important questions for the simulation of sedimenting discs include: Do the two discs descend at the same speed? Do they interact? If so, why, and under what conditions? How do the forces exerted on each disc influence its motion and how do they depend on their relative position? For any foam simulation: what effects do topological changes (T1s) have, and for how far do these effects extend?

3.5 Standard Methods for Foam Visualization

We identify the properties of the foam in which we are interested and the standard methods of visualizing the simulations using the constriction example.

Firstly, each bubble acts as a tracer, so its velocity, defined as the motion of the center of mass, provides traditional information about the flow: velocity vectors, trace streamlines and velocity components. In addition, each bubble has a well-defined pressure, which, when averaged over the duration of the simulation, can, as for velocity, be visualized using color mapping or slices across and along the flow direction. A further benefit of the use of bubbles as tracers is that their deformation gives information about the local strain. Quantities such as the texture tensor [11], which takes an average of distances between bubble centers in a given representative volume element, can also be displayed as color maps, slices, and ellipses. Finally, the skeletonized views of the foam can themselves be animated. Fig. 1 shows examples of standard visualizations used by the domain experts.

Standard animation of the foam skeleton makes the analysis and visualization of individual bubbles extremely difficult over many time steps. The standard averaging techniques do not provide very much detail and are not well suited for the simulation of sedimenting discs. Line graphs decouple important information from the space-time domain. We demonstrate how our visualizations address these drawbacks.

4 Foam Visualization

Our visualization solutions are driven by the foam research and visualization challenges listed in Section 1. Section 4.1 describes the processing required to read SE output files and access the complete data generated by the simulation. Our application works with any SE simulation and no changes to the simulation output are necessary to accommodate the application. This processing addresses challenge one.

Visualizations of individual time steps, done using color-mapped attribute values, are used as the basis for, or for augmenting, more complex visualizations. Color-mapped visualizations are enhanced with bubble selection, with histogram-guided color-bar clamping and with T1 information overlay that shows the topological changes (T1s) triggered in the current time step. Bubble selection and/or filtering is used for debugging (selection by bubble ID), for studying foam properties at certain locations in the domain (filtering by location) or for analyzing bubbles with certain attribute values (filtering by attribute value).

Overall foam behavior (challenge three) is analyzed using the image-based statistical computation and visualization (Section 4.2), and visualization of bubble paths (Section 4.4).

Foam scientists wish to understand what triggers certain behavior in foam simulations (challenge two). Different views provide different information about the various influences on foam behavior. We enable the examination of several views at the same time using the multiple linked-views (Section 4.5).

Histograms provide important information about foam data, are used for bubble selection based on the values of attributes, and for providing the context for color map clamping. They are presented in Section 4.6. Interaction operations including navigation, selection, filtering, encoding and connections between multiple linked-views [30] are described in Section 4.7. These features are used throughout the application and help to address both challenges two and three. Note that each simulation attribute uses its distinct color-map palette which is used consistently throughout the paper. We use diverging color maps [21]: blue-red for elongation, blue-tan for pressure and purple-orange for velocity.

4.1 Data Processing

In this section, we present the data processing applied before visualization. We parse Surface Evolver (SE) output files, then we unwrap geometric elements of the foam described by periodic boundary conditions. Additional processing includes calculation of derived attributes, bubbles' centers, bounding boxes and statistical measures. We acceler-

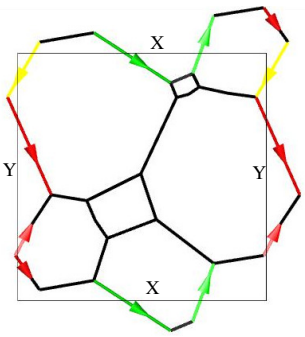

Fig. 3. Foam with periodic boundary conditions (PBC). The domain is shown as a black rectangle. A tessellation of the infinite plane can be obtained by tiling it with the domain. Edges that do not cross a domain boundary are shown in black. Edges that cross a domain boundary are colored depending on the boundary they intersect: red for the X boundary, green for the Y boundary and yellow for both X and Y boundaries. Arrows show whether an edge enters or exits the domain.

ate the data processing phase by parsing and pre-processing time steps in parallel on all available CPU cores.

4.1.1 Parsing

Foam simulation data consists of a list of SE output files, one per time step. A file stores the entire configuration of the simulated foam at a particular time step. For maximum generality and flexibility, we parse SE files directly instead of using derived files created by foam scientists. This allows our application to work with any simulation created using SE and at the same time it gives us access to the entire state of the simulation.

A Surface Evolver (SE) file [27] is organized into six parts: definitions and options, vertices, edges, faces, bodies and commands. The first section contains, in addition to options controlling the simulation, constant expressions for foam material and geometric parameters, additional attributes that are attached to geometric elements (vertices, edges, faces and bodies) and functions for defining level-set constraints. A level-set constraint is a restriction of vertices to lie on the zero level-set of a function. For instance, the foam container in the constriction dataset (Fig. 1 left-top) is defined using a level-set constraint. The lists of geometric elements (vertices, edges, faces and bodies) follow the format described next. Each line is comprised of entries which define an element. The first entry is the element ID followed by geometry data, followed by optional attributes. The geometry data consists of coordinates for a vertex, begin and end vertex for an edge, list of ordered edges for a face, and list of oriented faces for a body. Besides the built-in attributes for each element type, one may specify values for extra attributes. The commands section is used for controlling the simulation and it is ignored by our program.

Our tool can read the following optional data that is saved by the simulation code: a list of T1s and the network and pressure forces that act on a body. T1s are stored one per line. Each line contains the time step at which the T1 occurs, and the x and y coordinates of the T1. The network and pressure forces are stored component wise in SE variables.

4.1.2 Unwrapping for Periodic Boundary Conditions

After parsing foam simulation data and creating the corresponding data structures, we perform additional data processing. First we compact each list of geometric elements as there can be numbering gaps in the list specified in a SE file. Then, if the foam described in the SE file contains periodic boundary conditions (PBC) [27, 28] we unwrap the geometric elements so that we can display the foam.

For a foam with PBC, the domain boundary intersected by each directed edge and whether the edge enters or exits the domain (Fig. 3) is specified. All vertices are defined inside the domain. To unwrap edges, we use intersection information between an edge and a domain boundary. This may create vertices defined outside the domain. To unwrap faces, we follow connected edges along a face. This may create edges defined outside the domain.

4.1.3 Additional Processing

We calculate each bubble's center of mass, bounding box and the bounding box of the foam at each time step and overall, and calculate statistical quantities such as histogram, minima and maxima for values of attributes.

Algorithm 1 Align median pressure between time steps

Translate all pressures in a time step with a constant value such that the minimum pressure is zero.
Calculate the median pressure for each time step.
Calculate *maxMedian* the maximum of all medians.
Translate pressures in a time step with (*maxMedian* - median) for the time step.

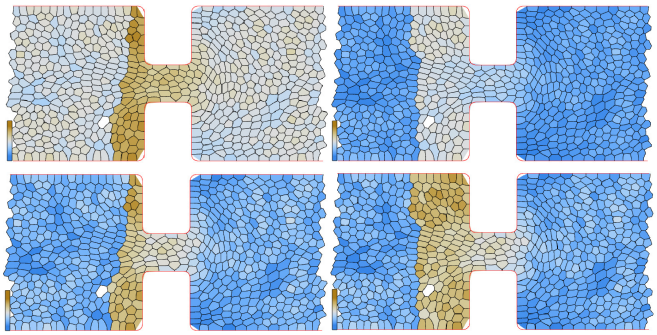

Fig. 4. Adjustment for relative pressure. Bubbles are color-mapped to pressure values. We show time steps $t = 26$ and $t = 27$: (top) before adjustment and (bottom) after adjustment. The white bubble is the reference bubble. A discontinuity in pressure values is present along the line of films that is moved downstream in each simulation step (Section 3.3).

Two important scalar attributes provided by the foam simulation are pressure and volume. We derive the following attributes important to foam scientists. Velocity, computed by connecting a bubble's center of mass between two consecutive time steps, and elongation, computed by $P/\sqrt{A}$ (in 2D) where P is the bubble's instantaneous perimeter and A is its area.

In SE simulations, there are high fluctuations of pressure values between successive time steps (Fig. 4 top). These fluctuations do not have any physical significance, but they are a consequence of the how pressure is recorded in the simulation files. We apply the processing in Algorithm 1 which eliminates pressure median variation and yields a smooth transition between time steps and a more meaningful representation of pressure (Fig. 4, bottom). SE records the pressure values of the bubbles relative to the pressure of a reference bubble, which is considered to have zero pressure. This is because to find the mechanical equilibrium state of the foam it is enough to calculate pressure *differences*, not absolute values. We started by calculating a bubble's center of mass assuming that its mass is concentrated in its vertices. However this results in bubbles that appear to wobble when their center is set stationary (Section 4.2). The reason for this is that many vertices on one side of a bubble will pull its center of mass toward that side. We solve this problem by computing the center of mass, assuming the mass is uniformly distributed on the bubble's area [1].

4.2 Image-based Statistical Computation and Visualization

Bubble-scale simulations can be too detailed for observing general foam behavior and T1 events generate large fluctuations in attribute values that hide the overall trends. A good way to smooth out these variations is to calculate the average of the scalar field over all time steps, or over a time window before the current time step. This visualization reveals global trends in the data because large fluctuations caused by T1s are eradicated. This results in only small variations between averaged successive time steps.

We take advantage of the graphics card capabilities to calculate a per-pixel average over all time steps for a given scalar field. Our solution is faster than a software solution and it is arguably simpler, as scan conversion of graphics primitives is done in hardware.

We use three floating point textures stored in three framebuffer objects: $\vec{step}$, $\vec{previous}$ and $\vec{current}$. Even though these are 2D textures, to simplify the presentation we use a 1D index to access a texel. We

Algorithm 2 Image-based statistical computation

Input: t_{Total} time step where we stop the statistical calculations, t_{Window} calculate the average for the last t_{Window} time steps behind t_{Total}

Output: average and count values for t_{Window} time steps behind t_{Total} are stored in $\vec{current}$. Minimum and maximum are calculated for all time steps t_{Total}.

```
t = 0; t_CurrentWindow = 0
Set every texel of current to (0, 0, max float, min float)
while t < t_Total do
    Render the foam for time step t into step, but store attribute values instead of colors.
    current = previous ⊕ step
    previous = current
    t_CurrentWindow = t_CurrentWindow + 1
    if t_CurrentWindow > t_Window and t >= t_Window then
        Render the foam for time step t − t_CurrentWindow into step, but store attribute values instead of colors.
        current = previous ⊖ step
        previous = current
        t_CurrentWindow = t_CurrentWindow − 1
    end if
    t = t + 1
end while
```

use index i between square brackets to denote the texel at index i. We use the field access notation from C++ to access component R, G, B or A of a texel. So, $\vec{v}[i].R$ would access component R of texel i of texture v. $\vec{previous}$ and $\vec{current}$ textures store the result for time steps $t < n$ and for $t \leq n$ respectively where n is the current time step. In each RGBA texel we store a sum of scalar values, a count that keeps track of how many values we have rendered over that texel, the minimum and the maximum values. Texture $\vec{step}$ stores an image similar to Fig. 4 but instead of colors it stores the actual scalar values. In our algorithm, we use two operations between textures: $\oplus$ adds the scalar values stored in R, increments the count stored in G and calculates the minimum and maximum for the values stored in B and A; $\ominus$ subtracts the scalar values stored in R and decrements the count stored in G. Our image-based statistical computation procedure is presented in Algorithm 2.

To visualize the statistical quantities calculated by Algorithm 2, we use a fragment shader to render the average, count, minimum or maximum depending on a variable passed to the shader. We map one of those values to color using a uni-dimensional texture. We only render texels that have the count ($\vec{current}[i].G$) non-zero.

A visualization of the per-pixel average for velocity magnitude and pressure over all time steps is shown in Fig. 5. Compared with typical visualizations (Fig. 1 left bottom) our solution is fast, high resolution and can use different color maps and clamping to emphasize features of interest.

Our application can generate an animation of the rolling average up to time step i where $i \in [1, n]$, and n is the number of time steps in the simulation. With this visualization, domain experts can observe, for the first time, the point at which the overall trends are clearly visible and when any transient behavior ends. This allows the determination of the optimal duration of a simulation such that it can capture the dynamics of the underlying phenomena. For instance, the rolling average animation (Fig. 5) shows that, for the constriction dataset, the calculated averages converge around time step 400, which means that very little change can be observed in the calculated averages beyond this time step.

4.2.1 Average around a moving body

For the simulation of sedimenting discs, the areas of interest are around each disc. A statistical calculation using a fixed world coordinate system (foam is stationary and the discs descend through it) would not produce useful results. To explain this (Fig. 6), let's say that we are interested in calculating the average in an area (small circle) situated at three o'clock adjacent to a disc (big circle) that descends

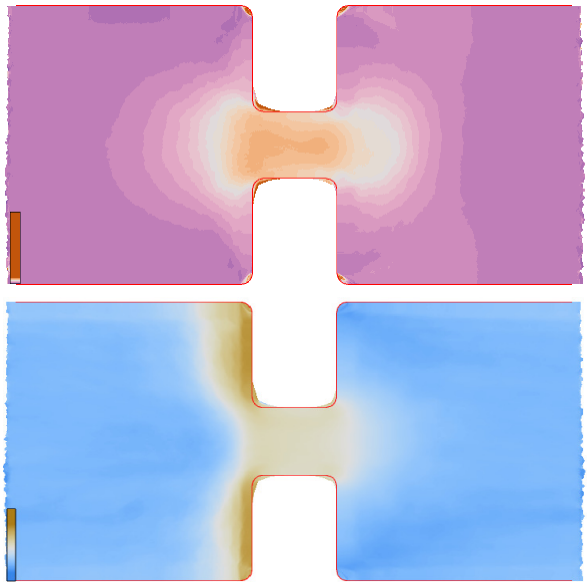

Fig. 5. Visualization of the per-pixel average of attribute values for all time steps of the simulation. We show the average of velocity magnitude (top) and pressure (bottom). The velocity is color-mapped using purple-orange divergent color map. Pressure is color-mapped using a blue-tan divergent color map (constriction simulation). Compare with Fig. 1.

through foam (rectangle) due to gravity. The disc is at two different positions p and q at time steps i and k. The interesting area relative to the disc also descends, so it is at positions b_{pi} and b_{qk}. Using a fixed world coordinate system, the average is calculated by overlapping the two foam images (rectangles) and then averaging the corresponding pixels in each image. This computation yields an incorrect formula for the area adjacent to the disc: $(b_{qi} + b_{qk})/2$. By using a fixed disc coordinate system (the disc is stationary and the foam flows around it), the average calculation changes to $(b_{pi} + b_{qk})/2$, the correct result.

4.2.2 Average around multiple moving bodies

If there are multiple moving bodies, as is the case for the simulation of sedimenting discs, we can obtain correct average values only around the disc that is set stationary. To see correct average values around multiple moving bodies we use our multiple linked-views feature. We display two views color-mapped by the same attribute and we set a different body stationary in each view. This way domain experts can study a correct sliding time window average around each body involved in the interaction. For a detailed description of the multiple linked-views feature see Section 4.5.

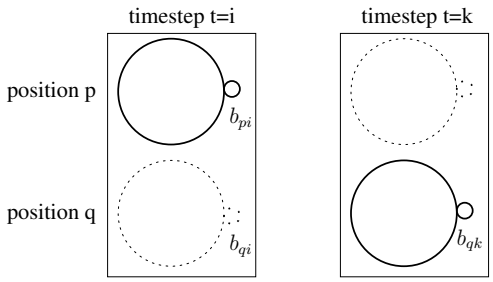

Fig. 6. Average computation for an area (small circle) around a sedimenting disc (big circle) descending through foam (rectangle). Future (for $t = i$) and past (for $t = k$) disc positions are represented with a dashed line. For a fixed world coordinate system (the foam is stationary and the disc falls through it), the average computation is incorrect $(b_{qi} + b_{qk})/2$). For a fixed disc coordinate system (the disc is stationary and the foam flows around it), the average computation is correct $((b_{pi} + b_{qk})/2)$.

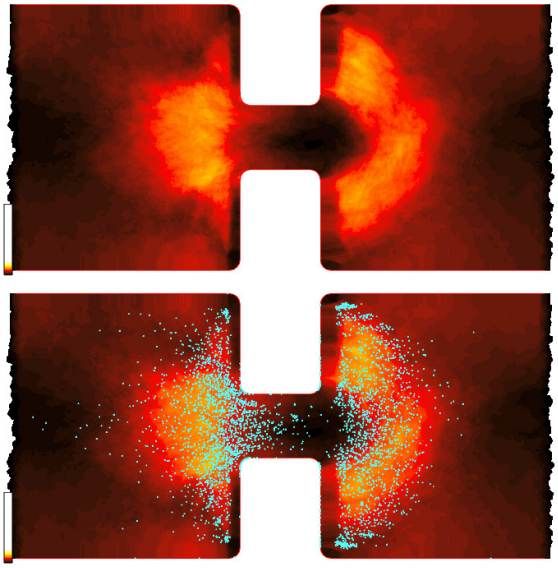

Fig. 7. Where do most bubbles with negative velocity along X occur? The top image shows the number of times a bubble with negative velocity along X covers a pixel. The range of the color map is 0 to the number of time steps 1000. The bottom image shows the same information overlayed with the location of T1s shown as cyan dots.

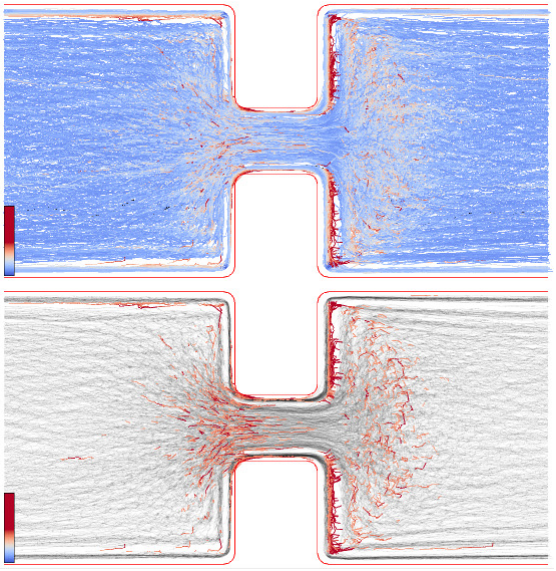

Fig. 8. Visualization of bubble paths. Path color is mapped to elongation. We show: (top) bubble paths along all time steps for all bubbles in the simulation and (bottom) trajectories that contain bubbles with elongation at least 80% of the maximum elongation (constriction simulation). We use a focus+context approach where the selections are color-coded and the context paths are semi-transparent grey-scale.

4.2.3 Sliding time window

Calculating the average over all time steps works well for the foam flow through a constriction. However that is not the case for the sedimenting discs simulation, because of the important transient state the discs go through. The two discs are initially side by side (Fig. 1 right, 13 top), they interact by rotating about one another (Fig. 13 middle) and they reach a steady state when a line connecting their centers becomes parallel to gravity (Fig. 13 bottom).

We provide a *sliding time window* user option which allows the calculation of average only for a specified number of time steps behind the current time step. This allows the study of the transient state the two discs go through while maintaining the advantages that averaging of values provide. The length of the sliding time window is a user supplied parameter that depends on the duration (number of time steps) of the transient state.

4.2.4 Domain histogram

We can use bubble selection by attribute value (Section 4.7) and the count computed together with other statistical values to answer the following question: Where in the domain do the most bubbles with attributes in a certain range of values occur? For instance, Fig. 7 shows where most bubbles with negative velocity along X occur. Those areas match well with the location of the T1s.

Our novel visualization solution led to insights into the following research questions: Why is a terminal separation of roughly two bubble diameters attained between the two discs once they have rotated about one another into a stable orientation? Why do discs drift laterally as they sediment? To simplify our presentation we show our findings using only one stationary body, instead of visualizing multiple moving bodies (Section 4.5), as in this case it makes no difference to the conclusion.

4.3 Force visualization

For the sedimenting-discs simulation, the network and pressure forces acting on each disc are saved by the simulation code. T1 events cause large fluctuations in the value and orientation of these forces, which can make analysis of the simulation data more difficult. To reduce the distraction of the fluctuations, we offer the possibility to smooth the forces over a time window before the current time step. These calculations are integrated with the image based average calculations (Section 4.2). Each force (instantaneous or average) acting on a disc is represented as a line segment that starts in the center of the disc and has length proportional to the magnitude of the force.

4.4 Visualization of Bubble Paths

Visualization of bubble paths complements the image-based statistical computation and visualizations by providing information about the trajectory of individual bubbles in the simulation. The paths are a useful way to compare simulation with experiment. They also provide insight into the overall behavior of the foam. A bubble path is determined by connecting the center of bubbles with the same ID in consecutive time steps. When a bubble exits the domain through a boundary edge, it enters the domain through the opposite boundary edge. Our software computes the correct path in this case.

Despite the problems associated with overlapping bubble paths, tracing all paths simultaneously still conveys useful information about foam behavior. Looking at Fig. 8 top, gaps where no bubble traverses reveal themselves. This tells us that when bubbles touch a wall they have a strong tendency to remain attached to it.

While the path visualization for all bubbles presents the overall behavior of the foam, overlapping paths prevent tracking the path of individual bubbles. We offer three solutions to solve this problem. We select paths based on location (Fig. 9). We can also select paths that include bubbles with attribute values in an interval specified in the histogram view. This way, we can observe not only the time step and bubbles that have certain values but the entire evolution of the selected bubbles. For instance, Fig. 8 bottom image shows the bubble paths for bubbles that reach at least 80% of the maximum elongation. A bubble's position when it is highly elongated is colored red and the rest of its path is semi-transparent grey. This visualization shows clearly that the bubbles are most elongated as they enter and after they exit the constriction. This corresponds well with regions where the velocity gradient is large (Fig. 5 top) and with the location of T1s (Fig. 7 bottom).

Three-dimensional bubble paths alleviate the problem of overlapping paths in 2D through lighting effects. They map time to height and enable multi-variate visualizations. We design 3D bubble paths by assigning each time step to a corresponding height. Consecutive time steps are assigned to adjacent heights, and all heights are equally spaced. Time steps 0, 1, 2, ... are assigned to heights 0, h, $2h$, ..., where h is a user specified parameter. Velocity is implicitly depicted

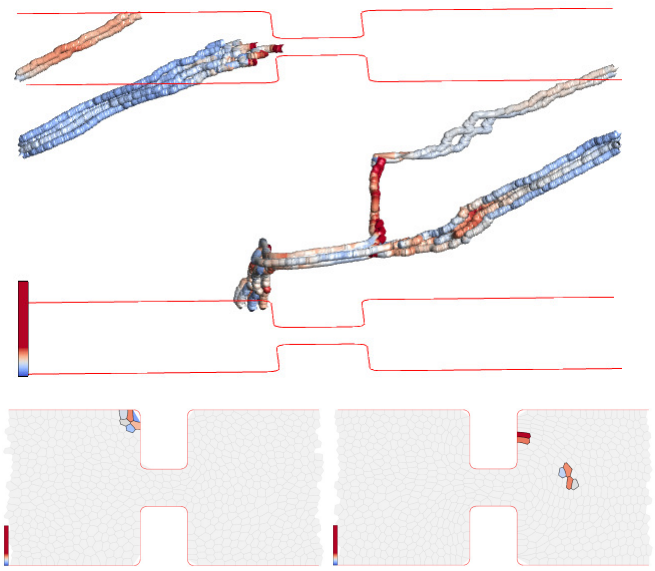

Fig. 9. 3D bubble paths. Bubble and path color is mapped to elongation. We show visualizations for bubbles that start in the corner upstream of the constriction: (top) 3D bubble paths and (bottom) time step visualizations (t=0, t=361). Vertical 3D bubble paths correspond to bubbles that do not move in the X direction. The two red (high elongation) bubbles in the bottom-right view are attached to the wall. The length of time they stay there is displayed as a vertical path in the top view.

in this representation. Paths of bubbles which are stationary will appear as vertical, while the higher the velocity of bubbles the closer to the horizontal their paths will appear. Paths can be color-mapped to any other attribute enabling comparison of velocity to other attributes.

We select bubbles upstream of the constriction (Fig. 9 bottom-left) and we visualize their paths using the 3D bubble paths visualization (Fig. 9 top). Two important behaviors stand out. First, long straight, vertical paths that correspond to bubbles that have zero velocity along the X direction. Those indicate bubbles that are in contact with the wall. As these bubbles have high elongation, they are colored red. Second, we notice long straight edges associated with sharp path angles. These indicate topological changes (T1s).

Of course rendering too many 3D bubble paths causes occlusion. Thus we can filter bubble paths based on any of their attributes such as velocity magnitude, pressure and elongation.

4.5 Multiple Linked-Views

Foam scientists wish to understand what triggers certain behavior in foam simulations, so the ability to see different attributes at the same time and to understand how different attributes relate to one another is very important. We provide up to four different linked-views [17, 24], which can depict any of the following views: a time step visualization, an average visualization or a bubble path visualization. For maximum flexibility, each view can depict a different attribute, uses its own color-bar and can show the navigation context. Additionally, a histogram view for one of the attributes can be displayed. The histogram is used for specifying a selection criteria on an attribute value. To set up optimal views to analyze data, users can copy viewing transformations and also copy the color mapping between views depicting the same attribute.

We provide two *connection operations* [30]: a time connection and linked-selection connection. Each view is linked to the same time step, as foam scientists want to understand what gives rise to certain effects when they are studying foam behavior. Linked-selection works by showing how data selected in one view appears in other views. This is used to see, for instance, the elongation of high pressure bubbles or both pressure and elongation for bubbles involved in a T1 event.

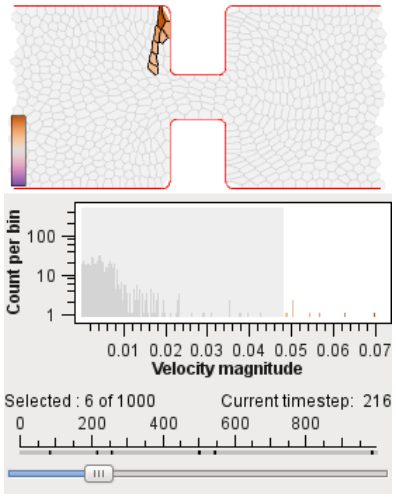

Fig. 10. Selection and filtering using the histogram tool. We select only bubbles with velocity magnitude values greater than 70% percent of the maximum. Only six time steps out of 1000 contain bubbles with these velocities and those time steps are indicated on the time slider.

4.6 Histograms

We provide both a histogram of bubble attribute values over one time step and over all time steps. To facilitate data analysis, our histogram is configurable. The user can choose a maximum height, logarithmic or linear height scale and uni-color or color-coded display. Histograms are also used in selection and filtering of data based on attribute value and in color-map clamping used for selecting features of interest in the data. These interactions are described in detail in Section 4.7.

4.7 Interaction

Interaction with the data is an essential feature of our application.

Navigation is used to select a subset of the data to be viewed, the direction of view, and the level of detail [30]. We provide the following navigation operations: rotation around a bounding box center for specifying the direction of view, and translation and scaling for specifying the subset of data and the level of detail. A navigation context (Fig. 14 left) insures that the user always knows its location and orientation during exploration of the data.

We can **select and/or filter** bubbles and center paths based on three distinct criteria: based on bubble IDs, to enable relating to the simulation files and for debugging purposes; based on location of bubbles (Fig. 2 and Fig. 9), to analyze interesting features at certain locations in the data; and based on an interval of attribute values specified using the histogram tool (Fig. 8 right and Fig. 10). A composite selection can be specified using both location and attribute values.

Selected bubbles or center paths constitute the focus of our visualization, and the rest of the bubbles or center paths provide the context [14]. The context of the visualization is displayed using user-specified semi-transparency, or it can be hidden altogether. Fig. 10 shows how selection and filtering is performed using the histogram tool. We select velocity magnitude values greater than 70% of the maximum (using a selection brush). Only six time steps out of 1000 contain bubbles with these velocities and those time steps are indicated on the time slider. The user can easily navigate to those time steps. The upper image shows one of those time steps, with bubbles with velocity greater than 70% in focus.

Encoding operations are variations of graphical entities used in a visualization that emphasize features of interest [30]. We provide encoding operations to change the color map used, to specify the range of values used in the color map and to adjust the opacity of the visualization context. Selection of the interval used in color-mapping is guided by the histogram tool (Fig. 11). This provides essential information for selecting an interval that reveals features of interest.

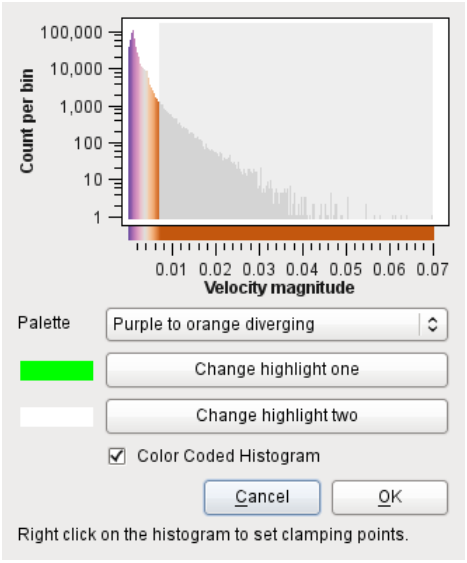

Fig. 11. Color-map clamping guided by the histogram tool. This is a histogram of the constriction simulation which uses the logarithmic height scale. This histogram shows that relatively few bubbles (determined by T1s) have high velocity.

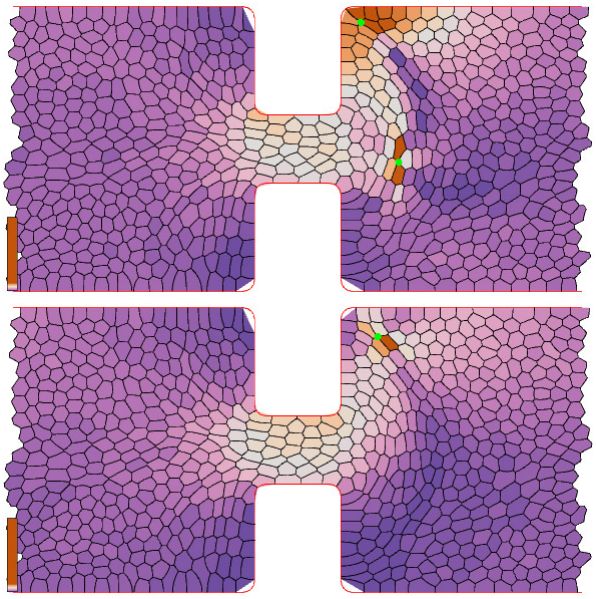

Fig. 12. High velocity bubbles outside the constriction are caused by T1 events (green dots). Time steps t=62, t=63 for the simulation of foam flow through a constriction. Bubbles are color-mapped to velocity magnitude. The color bar is clamped to about one tenth of its range to highlight the high velocity in the constriction area. The highest velocities are caused by T1 events.

4.8 Limitations and Drawbacks

Our system has the following limitations. Sending the data for 3D bubble paths (Section 9) to the graphics card is slow (a couple of seconds). Navigation operations are interactive afterwards.

Bubbles with vertices on level-set constraints (Section 4.1.1) are not accurately represented. Any bubble edge that lies on a constraint should be represented by the function described in the data file rather than the current approximation of a single line segment. This causes the artifacts visible at the corners in Fig. 5.

Our measure of elongation, $P/\sqrt{A}$, depends weakly on the number of sides of a bubble and, more importantly, does not indication the direction in which a bubble is elongated. We expect to address these limitations in a future version of the program.

5 Results

We present results and analysis obtained by domain scientists using our tool. The results presented in Section 5.3 and Section 5.4 require analysis of multiple moving bodies, which is done using the multiple linked-views and multiple stationary bodies. To simplify presentation of results for the sedimenting discs simulation, we describe our findings by setting only one body to be stationary.

5.1 High velocity bubbles outside the constrictions are caused by T1 events

An unexpected behavior of the foam detected in the simulations and shown by our visualizations is that the largest velocities are exhibited not when foam moves through the constriction but at what first appears as seemingly random times and positions (Figure 12).

For this reason the color bar is clamped at about one tenth of the total velocity magnitude range. Previously, foam scientists hypothesized that those high velocities are caused by topological changes (T1s). We can now verify this hypothesis by matching T1 positions with positions of high velocity bubbles. Fig. 11 shows, by using the velocity magnitude histogram, that only a few bubbles have very high velocity magnitude and determine the upper limit of the velocity magnitude range.

5.2 Why does one disc initially descend quicker than the other?

An important question foam scientists wish to answer relates to what triggers the interaction between the two discs in the simulation of sedimenting discs. That is, why does one disc initially descend quicker than the other? In Fig. 13 top, we see that the disc on the right trails the disc on the left as a result of the initial arrangement of the surrounding bubbles. For $t = 0$, the network force acts downwards for the disc on the left while the pressure force is negligible. However, both network and pressure forces act upwards for the disc on the right. The difference in the network force exerted on each disc is due to the different distribution of films in contact with each disc. Similarly, the difference in the pressure force exerted on each disc is due to the differences in the shapes of bubbles in contact with each disc. As a result, the disc on the right is left behind. It is the initial configuration of the foam that decides which disc gets left behind (the disc on the right in the case shown).

5.3 Why is a terminal separation of roughly two bubble diameters attained between the two discs?

To answer this question, we investigate the shape of bubbles between the discs once they have reached this separation. Using a sliding time window average of bubble elongation over 10 iterations, we observe a competition between the effects imposed by each disc on the foam. We expect bubbles in front of the trailing disc to be compressed and bubbles in the wake of the leading disc to be stretched, so their elongation is high in both cases. However, it can be seen in Fig. 13 bottom-left that the competition between the stresses applied by each disc results in a lower than expected deformation of the foam occurring between the two discs. This competition results in the bubbles in-between the two discs remaining (roughly speaking) undeformed. As a result, the forces experienced by each disc become similar. A terminal separation of two bubbles is attained between the two discs, although why this is two and not, say, one or three is a question to which we will return in future work.

5.4 Why do discs drift laterally as they sediment?

To gain insight into this question, we consider how the pressure and elongation field of the foam evolves as the discs descend. It could be seen from previous visualizations of individual time steps that the pressure field is not symmetric during the rotation of the two discs about one another. This is validated by images produced using image-based statistical calculation and visualization, the *sliding time window* and *stationary body* features in FoamVis (Fig. 13 middle and bottom).

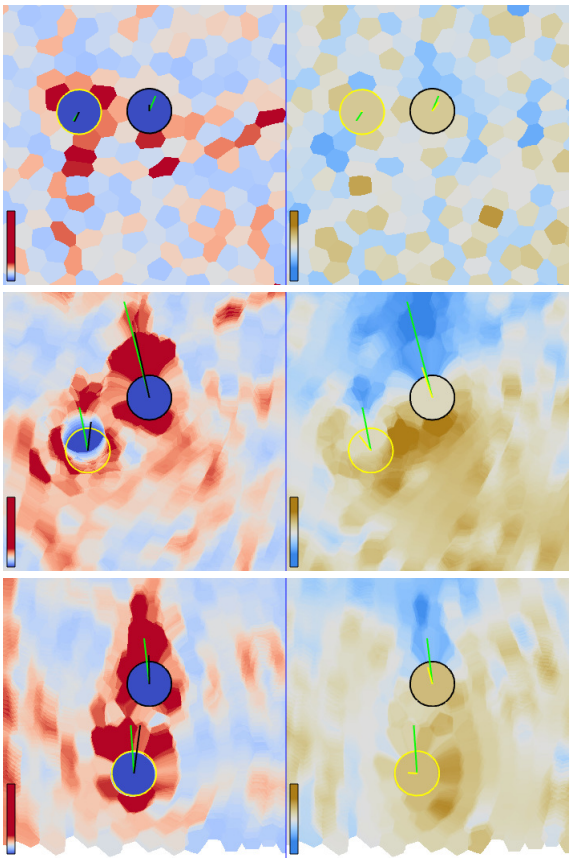

Fig. 13. Three time steps in the sedimenting-discs simulation: (top) Beginning of the simulation $t = 0$. (middle) The discs rotate about one another, $t = 43$; (bottom) Behavior near the end of the simulation, where the stable orientation of the discs is approached, $t = 246$. Each time step contains two views: with bubbles color-mapped to elongation (blue-red palette) and pressure (blue-tan palette). For time steps $t = 43$ and $t = 246$ we show a sliding time window average over 10 iterations for both scalar fields and forces. The stationary disc is marked with a black circle and the moving disc is marked with a yellow circle. We use black for the network force, yellow for the pressure force and green for the resultant force (pressure + network force) that acts on a disc. Note the incorrect average calculation around the moving disc (yellow circle) with high velocity (middle).

Here, it is observed that a region of higher pressure occurs to the right of both discs during their descent. The deformation of the foam is such that bubble pressures contribute to the drift of the discs as they sediment.

We can also observe that the network force initially contributes to forcing the rear disc to move laterally (Fig. 13 middle-left). However, once the discs have moved closer to their stable orientation, it is the pressure force that is driving the lateral drift (Fig. 13 bottom).

5.5 Pattern of bubbles traversing loops

For two discs sedimenting through a foam, our paths visualization shows that bubbles traverse loops to provide space for the descending discs. This behavior is not observed in standard visualizations used by the domain scientists. Fig. 14 left shows bubble paths color-mapped to velocity along the Y axis, with orange showing downward velocity and purple showing upward velocity. The orange area of high velocity along the Y direction shows the paths of the two discs, and the black rectangle marks the region magnified in the right image. A loop consists of a downward segment (colored orange) and an upward loop (colored purple). A bubble traverses the downward segment as a descending disc approaches it. Then it traverses the upward loop as the disc passes by it. The bubble avoids the falling disc and then fills the space that it leaves.

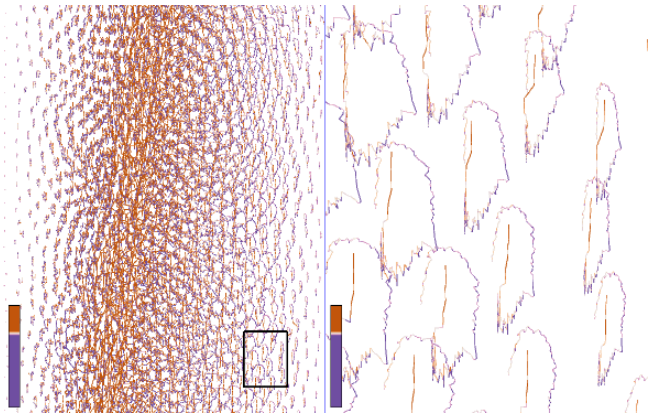

Fig. 14. Pattern of bubbles traversing loops not previously observed by domain experts. The bubbles paths are color-mapped to velocity along Y, with orange indicating descent and purple indicating ascent. The left image shows the bubble paths over the entire simulation. The red area shows paths of the two discs. The black rectangle shows the region that is magnified in the right image.

6 Conclusions and Future Work

We described the foam research application area and we presented a novel application that provides various techniques for the exploration, analysis, and visualization of foam simulation data. Our tool validates previous hypothesis and yields a more convenient representation of simulation data. Application scientists using our tool make new discoveries and gain insight into foam behavior. Based on the many research questions that domain experts are able to address, we believe we provide a valuable tool for visualization and analysis of data in the foam research community.

We believe there are many opportunities for future contributions of visualization to foam research. In the future, we want to create a composite image describing attribute averages around several moving objects, include other measures of elongation such as the texture tensor [11] and provide visualizations for 3D foam simulations.

Acknowledgments

SJC acknowledges financial support from EPSRC/P&G grant EP/F000049/1 and EPSRC grant EP/D071127/1. This research was supported in part by the Research Institute of Visual Computing (rivic.org) Wales. We thank Ken Brakke for answering our many questions about the Surface Evolver.

References

[1] G. Bashein and P. R. Detmer. Centroid of a polygon. In *Graphics Gems IV*, pages 3–6. Morgan Kaufmann, 1994.

[2] J. Bigler, J. Guilkey, C. Gribble, C. Hansen, and S. Parker. A Case Study: Visualizing Material Point Method Data. *EG Computer Graphics Forum*, pages 299–306, 2006.

[3] L. Bragg and J. Nye. A dynamical model of a crystal structure. *Proc. R. Soc. Lond.*, A190:474–481, 1947.

[4] K. Brakke. The Surface Evolver. *Experimental Mathematics*, 1(2):141–165, 1992.

[5] K. Chiang and W. Chen. Electronic packaging reflow shape prediction for the solder mask defined ball grid array. *Transactions-American Society of Mechanical Engineers Journal of Electronic Packaging*, 120:175–178, 1998.

[6] S. Cox and E. Whittick. Shear modulus of two-dimensional foams: The effect of area dispersity and disorder. *Eur. Phys. J. E*, 21:49–56, 2006.

[7] I. T. Davies. *Sedimentation of circular and elliptical objects in a two-dimensional foam*. PhD thesis, Aberystwyth University, 2009.

[8] M. Dennin. Discontinuous jamming transitions in soft materials: coexistence of flowing and jammed states. *J. Phys.: Condens. Matt.*, 70:283103, 2008.

[9] A. Glassner. Soap Bubbles: Part 1. *Computer Graphics and Applications, IEEE*, 20(5):76 –84, sep/oct 2000.

[10] A. Glassner. Soap bubbles: Part 2 [computer graphics]. *Computer Graphics and Applications, IEEE*, 20(6):99 –109, nov/dec 2000.

[11] F. Graner, B. Dollet, C. Raufaste, and P. Marmottant. Discrete rearranging disordered patterns, part I: Robust statistical tools in two or three dimensions. *Eur. Phys. J. E*, 25:349–369, 2008.

[12] M. Hadwiger, F. Laura, C. Rezk-Salama, T. Höllt, G. Geier, and T. Pabel. Interactive Volume Exploration for Feature Detection and Quantification in Industrial CT Data. *Visualization and Computer Graphics, IEEE Transactions on*, 14(6):1507–1514, 2008.

[13] K. Harsh, V. Bright, and Y. Lee. Solder Self-Assembly for Three-Dimensional Microelectromechanical Systems. *Sensors and Actuators A: Physical*, 77(3):237–244, 1999.

[14] H. Hauser. Generalizing Focus+context Visualization. *Scientific visualization: The visual extraction of knowledge from data*, pages 305–327, 2006.

[15] S. Jones, B. Dollet, N. Slosse, Y. Jiang, S. Cox, and F. Graner. Two-dimensional constriction flows of foams. *Colloids and Surfaces A: Physicochemical and Engineering Aspects*, 382(1-3):18 – 23, 2011.

[16] G. Katgert, M. Möbius, and M. van Hecke. Rate dependence and role of disorder in linearly sheared two-dimensional foams. *Phys. Rev. Lett.*, 101:058301, 2008.

[17] J. Kehrer, F. Ladstadter, P. Muigg, H. Doleisch, A. Steiner, and H. Hauser. Hypothesis Generation in Climate Research with Interactive Visual Data Exploration. *Visualization and Computer Graphics, IEEE Transactions on*, 14(6):1579–1586, Nov.-Dec. 2008.

[18] A. König, H. Doleisch, A. Kottar, B. Kriszt, and E. Gröller. AlVis-An Aluminium-Foam Visualization and Investigation Tool. In *Visualization (VisSym), EG/IEEE TCVG Symposium on*. Amsterdam, The Netherlands, 2000.

[19] D. R. Lipşa, R. S. Laramee, S. J. Cox, J. C. Roberts, and R. Walker. Visualization for the Physical Sciences. In *Eurographics*, LLandudno, Wales, UK, 12-15 April 2011. State-of-the-Art Reports.

[20] F. Losasso, J. Talton, N. Kwatra, and R. Fedkiw. Two-Way Coupled SPH and Particle Level Set Fluid Simulation. *Visualization and Computer Graphics, IEEE Transactions on*, 14(4):797 –804, 2008.

[21] K. Moreland. Diverging Color Maps for Scientific Visualization. In *Advances in Visual Computing (ISVC), International Symposium*, pages 92–103. Springer, 2009. additional online material, accessed Aug. 2010, `http://www.cs.unm.edu/~kmorel/documents/ColorMaps/index.html`.

[22] J. Plateau. *Statique Expérimentale et Théorique des Liquides Soumis aux Seules Forces Molécularies*. Paris: Gauthier-Villars, 1873.

[23] M. Rayner, G. Trägårdh, C. Trägårdh, and P. Dejmek. Using the Surface Evolver to Model Droplet Formation Processes in Membrane Emulsification. *Journal of colloid and interface science*, 279(1):175–185, 2004.

[24] J. Roberts. State of the art: Coordinated multiple views in exploratory visualization. In *Coordinated and Multiple Views in Exploratory Visualization, 2007. CMV '07. Fifth International Conference on*, pages 61 –71, July 2007.

[25] R. Shimada, S. Rahman, and Y. Kawaguchi. Simulating the Coalescence and Separation of Bubble and Foam by Particle Level Set Method. In *Computer Graphics, Imaging and Visualisation, 2008. CGIV '08. Fifth International Conference on*, pages 18 –22, 2008.

[26] C. Smith. Grain shapes and other metallurgical applications of topology. In *Metal Interfaces*, pages 65–108. American Society for Metals, Cleveland, OH, 1952.

[27] The Surface Evolver, Jan. 2008. Online document, accessed 29 Nov. 2010, `http://www.susqu.edu/brakke/evolver/html/evolver.htm`.

[28] Surface Evolver Workshop, Apr. 2004. Online document, accessed 1 Dec. 2010, `http://www.susqu.edu/brakke/evolver/workshop/workshop.htm`.

[29] R. Ďurikovič. Animation of Soap Bubble Dynamics, Cluster Formation and Collision. *EG Computer Graphics Forum*, 20(3):67–75, 2001.

[30] M. Ward, G. Grinstein, and D. Keim. *Interactive Data Visualization. Foundations, Techniques, and Applications*, chapter 10, pages 315–334. A K Peters, Ltd., Natick, Massachussetts, 2010.

[31] D. Weaire and S. Hutzler. *The physics of foams*. Oxford University Press, USA, 2001.

[32] A. Wyn. *Topological changes in sheared two-dimensional foams*. PhD thesis, Institute of Mathematics & Physics, Aberystwyth University, 2009.